

Anisotropic heavy Fermi-liquid formation in the valence fluctuating α -YbAlB₄

Yosuke Matsumoto,^{1,*} K. Kuga,¹ T. Tomita,^{1,†} Y. Karaki,^{1,2} and S. Nakatsuji^{1,‡}

¹*Institute for Solid State Physics, University of Tokyo, Kashiwa, Chiba 277-8581, Japan*

²*Faculty of Education, University of the Ryukyus, Nishihara, Okinawa 903-0213, Japan*

(Dated: May 31, 2022)

α -YbAlB₄ is the locally isostructural polymorph of β -YbAlB₄, the first example of an Yb-based heavy fermion superconductor which exhibits pronounced non-Fermi-liquid behavior above T_c . Interestingly, both α -YbAlB₄ and β -YbAlB₄ have strongly intermediate valence. Our single crystal study of the specific heat, magnetization and resistivity has confirmed the Fermi liquid ground state of α -YbAlB₄ in contrast with the quantum criticality observed in β -YbAlB₄. Both systems exhibit Kondo lattice behavior with the characteristic temperature scale $T^* \sim 8$ K in addition to a valence fluctuation scale ~ 200 K. Below T^* , α -YbAlB₄ forms a heavy Fermi liquid state with an electronic specific heat coefficient $\gamma \sim 130$ mJ/mol K² and a large Wilson ratio more than 7, which indicates ferromagnetic correlation between Yb moments. A large anisotropy in the resistivity suggests that the hybridization between $4f$ and conduction electrons is much stronger in the ab -plane than along the c -axis. The strongly anisotropic hybridization as well as the large Wilson ratio is the key to understand the unusual Kondo lattice behavior and heavy fermion formation in mixed valent compounds.

PACS numbers: 71.27.+a, 71.28.+d, 75.20.Hr, 75.30.Mb

I. INTRODUCTION

$4f$ based heavy fermion (HF) systems have attracted much attention with interesting phenomena such as unconventional superconductivity and non-Fermi-liquid (NFL) behavior found in the vicinity of quantum critical points¹⁻⁶. Our recent studies have found the first Yb ($4f^{13}$) based HF superconductivity with the transition temperature $T_c = 80$ mK in the new compound β -YbAlB₄^{7,8}. Pronounced NFL behavior above T_c and its magnetic field dependence indicate that the system is a rare example of a pure metal that displays quantum criticality at ambient pressure and close to zero magnetic field⁷. Furthermore, the T/B scaling found in our recent high-precision magnetization measurements clarifies its unconventional zero-field quantum criticality without tuning⁹, which can not be explained by the standard theory based on spin-density-wave fluctuations¹⁰⁻¹². In contrast to the canonical quantum critical materials, hard X-ray photoemission spectroscopy (HXPES) measurements have revealed strongly intermediate valence of Yb^{+2.75}, providing the only example of quantum criticality in a mixed valent system¹³. Whether the valence fluctuation is relevant for the mechanism of the quantum criticality and superconductivity is an interesting open question.

In this paper, we present the results of the specific heat, magnetization and resistivity measurements of α -YbAlB₄, the locally isostructural polymorph of β -YbAlB₄ with different arrangement of distorted hexagons made of Yb atoms (space group: $Pbam(\alpha\text{-YbAlB}_4)$, $Cmmm(\beta\text{-YbAlB}_4)$)^{14,15}. According to the HX-PES measurement¹³, α -YbAlB₄ also has an intermediate valence of Yb^{+2.73}. The results indicate a Fermi liquid (FL) ground state for α -YbAlB₄ in contrast to the unconventional quantum criticality observed in β -YbAlB₄. Interestingly, both systems exhibit Kondo lattice behavior

with a small renormalized temperature scale of $T^* \sim 8$ K although both of them have a large valence fluctuation scale of ~ 200 K. Below T^* , α -YbAlB₄ forms a heavy Fermi liquid state with an electronic specific heat coefficient $\gamma \sim 130$ mJ/mol K² and a large Wilson ratio more than 7, which indicates ferromagnetic correlation between Yb moments. Kadowaki-Woods ratio is found similar to those found in the normal Kondo lattice systems and considerably larger than mixed valent systems. Furthermore, a large anisotropy observed in the resistivities of α -YbAlB₄ suggests strongly anisotropic hybridization between $4f$ and conduction electrons. This strong anisotropy in the hybridization is the key to understand the mechanism of the heavy fermion formation as well as the Kondo lattice behavior found in the intermediate valence system. Partial information has already been discussed in Ref.¹⁶.

II. EXPERIMENTAL

High purity single crystals of α -YbAlB₄ were grown by a flux method¹⁵. Energy dispersive X-ray (EDX) and induction coupled plasma (ICP) analyses found no impurity phases, no inhomogeneities and a ratio Yb:Al of 1:1. Surface impurities were carefully removed with dilute nitric acid before measurements. We succeeded in growing pure crystals with residual resistivity ratio (RRR) up to 110. The magnetization M at $T > 2$ K was measured by a commercial SQUID magnetometer using pure single crystals (RRR ~ 50) of 2.4 mg. The magnetization data at $T < 4$ K and $B < 0.05$ T were obtained by using a high precision SQUID magnetometer installed in a ³He-⁴He dilution refrigerator⁹. The specific heat C of pure single crystals (1.1 mg, RRR ~ 50) was measured at temperature range $0.4 < T < 200$ K by a relaxation method

using a physical property measurement system. Four-terminal resistivity measurements were made by using a DC method ($300 \text{ K} \gtrsim T \gtrsim 0.5 \text{ K}$) and an AC method ($1.4 \text{ K} \gtrsim T \gtrsim 35 \text{ mK}$).

III. RESULTS AND DISCUSSION

First, we present the magnetic part of the specific heat C_m divided by temperature in Fig. 1 (a). C_m was obtained by subtracting the specific heat of α -LuAlB₄ shown in the same figure. Here, α -LuAlB₄ is the non-magnetic isostructural counterpart of α -YbAlB₄. The Debye temperature of α -LuAlB₄ is estimated to be 380 K from the T^3 dependence of C below 10 K. In both α - and β -YbAlB₄, C_m/T is strongly enhanced to be $\gtrsim 130 \text{ mJ/molK}^2$ in the low T limit, which is large compared to ordinary valence fluctuating materials, such as CeSn₃¹⁷ and YbAl₃¹⁸ (see Fig. 1 (a)) and is two orders magnitude larger than the band calculation estimates ($\sim 6 \text{ mJ/molK}^2$)^{19,20}. While clear $\ln T$ divergent behavior is observed in β -YbAlB₄ in the temperature range of $0.2 \text{ K} < T < 20 \text{ K}$, C_m/T in α -YbAlB₄ nearly saturates at $T < 1 \text{ K}$, indicating a Fermi liquid ground state. On the other hand, at higher temperatures above 10 K, C_m/T in α -YbAlB₄ merges to the $\ln T$ behavior of β -YbAlB₄. Fitting the $\ln T$ behavior of β -YbAlB₄ to $C_m/T = S_0/T_0 \ln(T_0/T)$ yields $T_0 = 180 \pm 10 \text{ K}$ and $S_0 = 3.7 \pm 0.1 \text{ J/molK}$ for β -YbAlB₄⁹. Here, T_0 provides a characteristic hybridization scale for the system and is close to the coherence temperature of 250 K set by the resistivity peak⁷. Another rough estimate of T_0 can be made using the temperature where the magnetic part of the entropy S_m reaches $R \ln 2$ (the entropy of a ground state doublet). In this way, T_0 for α -YbAlB₄ can be estimated to be $T_0 \sim 160 \pm 20 \text{ K}$, as shown in Fig. 1 (b). In order to obtain S_m , we assume a constant value of C_m/T (127 mJ/molK^2) below the lowest temperature of the measurements 0.4 K. These large values of T_0 are consistent with the intermediate valence of these systems because mixed-valent compounds are typically characterized by a much higher value of T_0 than Kondo lattice systems^{6,21,22}. A proposed crystalline electric field (CEF) level scheme, which reproduces the magnetic susceptibility, suggests a CEF level splitting of $\Delta = 80 \text{ K}$ ¹⁹. However, a Schottky peak of this level splitting which would appear at $\sim 25 \text{ K}$ with a height of $130 \text{ mJ/K}^2\text{mol}$ is not seen here. This is probably because the CEF levels are smeared out by the valence fluctuations.

The temperature dependence of the d.c. magnetic susceptibility $\chi = M/B$ are shown in Fig. 1 (c). Both systems exhibit strong Ising anisotropy with the strongly T dependent c -axis χ and almost T independent χ along the ab -plane¹⁵. Broad peaks found around 200 K in χ_{ab} for both systems (Fig. 2) are close to the T_0 scale obtained from C_m and the coherence temperature of the resistivity which we will discuss later. The c -axis component for both systems shows almost the same temper-

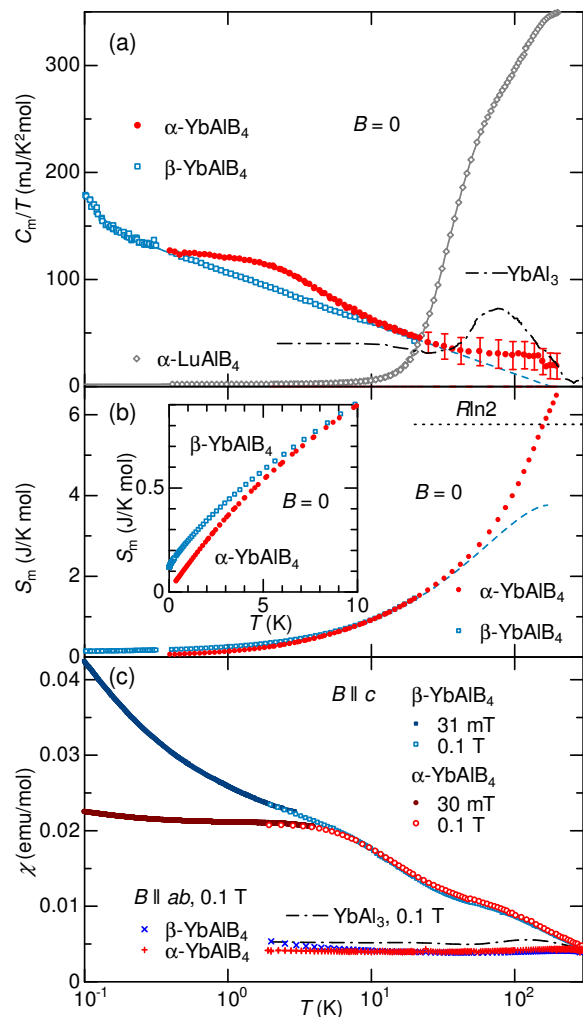


FIG. 1: (a) Magnetic part (f -electron contribution) of the specific heat C_m plotted as C_m/T versus T for both β - and α -YbAlB₄ under zero field. C_m/T for the β phase shows a $\ln T$ dependence for $0.2 \text{ K} < T < 20 \text{ K}$ ⁹. The broken line is the fit of the results to $C_m/T = S_0/T_0 \ln(T_0/T)$ (see text). C/T of α -LuAlB₄ and C_m/T of the intermediate valent cubic system YbAl₃¹⁸ are also shown. (b) The magnetic part of the entropy S_m , which was obtained by integrating C_m/T . In α -YbAlB₄, a constant value of $127 \text{ mJ/K}^2\text{mol}$ is assumed below 0.4 K. Above 10 K, C_m/T in α -YbAlB₄ merges to the $\ln T$ behavior of β -YbAlB₄. Thus the data for β -YbAlB₄ was shifted to take the same value as the one of α -YbAlB₄ at 20 K. The broken line is obtained from the $\ln T$ fitting used in (a). Inset shows the low T part. (c) Temperature dependence of the d.c. susceptibility $\chi = M/B$ measured in a field along the ab plane and c -axis for both β - and α -YbAlB₄. χ of the intermediate valent cubic system YbAl₃¹⁸ is also shown.

ature dependence down to $T \sim 8 \text{ K}$. Below $T \lesssim 8 \text{ K}$, on the other hand, these two systems show contrasting behavior: while β -YbAlB₄ continues to diverge due to the quantum criticality⁹, α -YbAlB₄ shows saturating behavior, indicating the Fermi liquid formation. The Curie-Weiss behavior, $\chi_c = C/(T+\Theta_W)$, is observed at $T > 150$

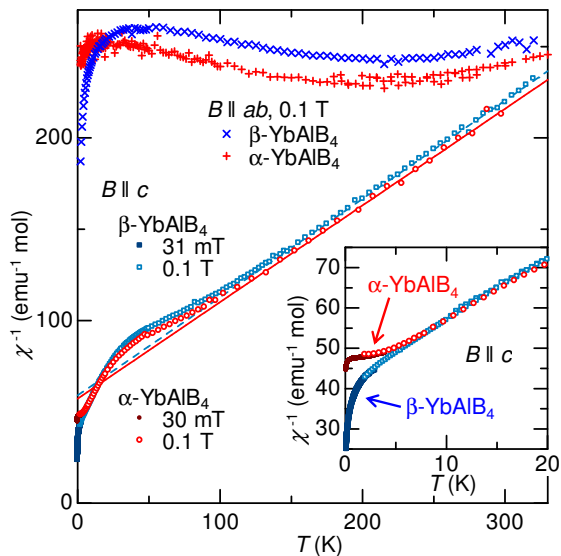


FIG. 2: Temperature dependence of the inverse susceptibility $\chi^{-1} = B/M$ under the field along the the ab -plane and c -axis. Solid and broken lines are Curie-Weiss fits above 150 K for α - (open circles) and β -YbAlB₄ (open squares), respectively. Inset shows the low temperature part of χ^{-1} under the field along the the c -axis.

K with $\Theta_W = 110 \pm 2$, 108 ± 5 K for α and β phases, respectively (Fig. 2). Ising moments $I_z = 2.22$, $2.24 \mu_B$ for α and β phases are deduced from the Curie constant $C = N_A I_z^2 / k_B$ where N_A and k_B are Avogadro and Boltzmann constants, respectively. Furthermore, at $T < 20$ K, another Curie-Weiss behavior is observed (Fig. 2 inset). If we fit the data to the Curie-Weiss law at $6 \lesssim T \lesssim 15$ K, $\Theta_W = 29$, 25 K and $I_z = 1.4$, $1.3 \mu_B$ are obtained for the α and β phases, respectively.

These observations suggest existence of local moments far below $T_0 \sim 200$ K possibly down to ~ 8 K. This Kondo lattice behavior with a low temperature scale $T^* \sim 8$ K is striking compared with ordinary valence fluctuating materials where Pauli paramagnetism is normally expected, such as CeSn₃²³ and YbAl₃¹⁸ (see Fig. 1 (c)). One of the possible origins of this behavior may lie in Kondo resonance narrowing²⁴ due to the presence of ferromagnetic (FM) interactions between Yb $4f$ -electron spins where FM interactions cause a large downward renormalization of the Kondo temperature from $T_0 \sim 200$ K to $T^* \sim 8$ K⁹. Indeed, the Wilson ratio $R_W = (\pi^2 k_B^2 / \mu_0 I_z^2) (\chi / \gamma) \sim 7$ is obtained for both α and β phases by using χ_c at $B = 0.1$ T, $T = 0.4$ K, $\gamma = C_m / T$ at $B = 0$, $T = 0.4$ K and I_z obtained from the high temperature Curie-Weiss fit. The R_W values are considerably large compared with the normal value 2 expected for Kondo lattice systems. If we use I_z obtained from the low temperature Curie-Weiss fit, the Wilson ratio becomes $R_W \sim 25$ for both systems, these significantly high values can be regarded as a consequence of the FM correlations.

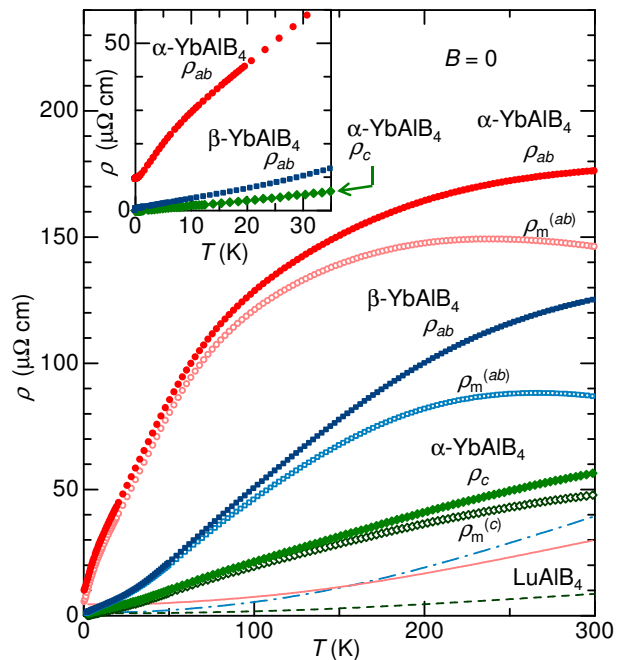


FIG. 3: Temperature dependence of the in-plane and c -axis resistivity ρ_{ab} and ρ_c of α -YbAlB₄ and ρ_{ab} of β -YbAlB₄. The magnetic part of the resistivity ρ_m is obtained by subtracting non-magnetic contribution estimated by ρ_{ab} of α -, β -LuAlB₄ (solid and dash dotted lines, respectively) or ρ_c of α -LuAlB₄ (dashed line). Inset shows low T part of ρ_{ab} and ρ_c .

Alternatively, the large R_W values might also be explained by the possible proximity to a valence quantum criticality as it have been recently pointed out by Watanabe and Miyake²⁵. In this case, the low temperature scale $T^* \sim 8$ K might arise from the characteristic energy scale for the valence fluctuations and not from the Kondo resonance narrowing. So far, we do not have experimental evidence to uniquely specify the mechanism among the possible scenarios. Further studies are required to solve this issue.

The temperature dependence of the in-plane resistivity with current along $[-110]$ direction, which we denote ρ_{ab} , and c -axis resistivity ρ_c are shown in Fig. 3. We have also measured the a -axis resistivity ρ_a and have found no significant difference from ρ_{ab} . This is consistent with the the recent band calculation²⁶, which predicts a nearly isotropic transport within the plane. Further investigation of the in-plane anisotropy including the b -axis resistivity ρ_b is now underway. Note that ρ_c in β -YbAlB₄ is not available so far due to the tiny thickness of $\sim 10 \mu\text{m}$ along the c -axis of single crystals. The magnetic part of the resistivity ρ_m is obtained by subtracting the corresponding component of ρ of the non-magnetic analog α - or β -LuAlB₄. The in-plane magnetic component, $\rho_m^{(ab)}$, exhibits broad peaks at $T \sim 250$ K in both α -YbAlB₄ and β -YbAlB₄, which are close to the peak temperatures of $\chi_{ab}(T)$ and T_0 obtained from C_m . Therefore, these may

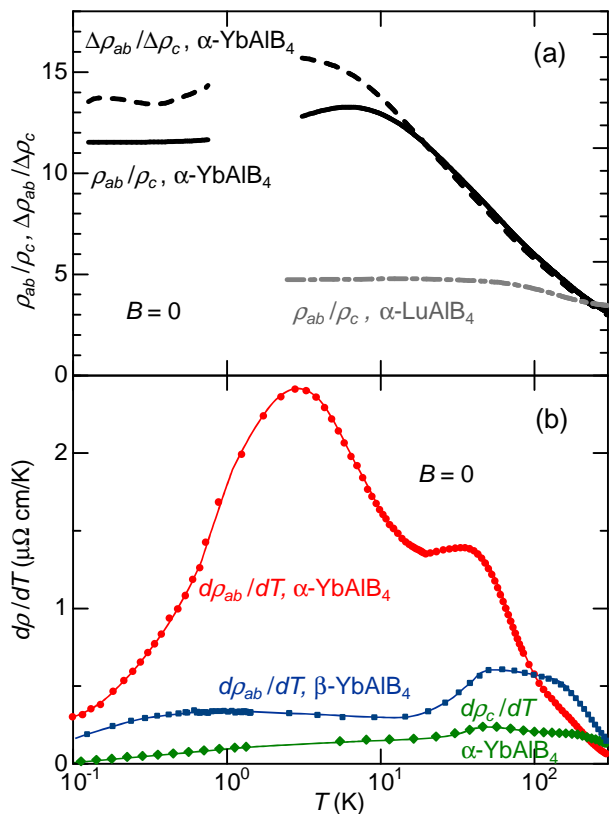


FIG. 4: (a) Temperature dependence of the ratio ρ_{ab}/ρ_c and $\Delta\rho_{ab}/\Delta\rho_c$. Here $\Delta\rho$ is defined by $\Delta\rho \equiv \rho - \rho_0$ (see text). (b) Temperature derivative of the resistivity $d\rho/dT$.

be considered as the coherence peak providing the characteristic hybridization temperature scale. On the other hand, $\rho_m^{(c)}$ in α -YbAlB₄ decreases monotonously on cooling below 300 K.

Interestingly, ρ_c is much smaller than ρ_{ab} in α -YbAlB₄ *i.e.* the conductivity of the system exhibits quasi-1D anisotropy. The ratio, ρ_{ab}/ρ_c , increases at low temperatures making a peak at $T \sim 6$ K (Fig. 4 (a), solid black line). At the peak, ρ_{ab}/ρ_c reaches ~ 13 and approaches to a constant value of ~ 11 in the lowest temperatures. This low temperature anisotropy is one order of magnitude larger than typical anisotropic heavy fermion systems such as CeCoIn₅²⁷, CeCu₂Si₂²⁸, CeNiIn²⁹, YbAgGe³⁰ where the ratio is almost T independent and $\lesssim 3$ below 300 K. On the other hand, ρ_{ab}/ρ_c in α -LuAlB₄ is nearly temperature independent with a slight increase from 3.5 at 300 K to 4.8 at lowest temperatures (Fig. 4 (a), dotted broken gray line). This temperature independent anisotropy in α -LuAlB₄ should come from the anisotropy of the Fermi surface. Interestingly, at $T \sim 300$ K, ρ_{ab}/ρ_c in α -YbAlB₄ approaches to a similar value to the one in α -LuAlB₄ although f electron contribution is dominant in α -YbAlB₄. This suggests that the topology of the Fermi surfaces of these systems are similar to each other at high $T > T_0$.

The peak found in ρ_{ab}/ρ_c arises mainly from a rapid decrease in ρ_{ab} below $T \sim 10$ K (Fig. 3 inset). This can be clearly seen in the temperature derivative of ρ , $d\rho/dT$ shown in Fig. 4 (b). While $d\rho_c/dT$ is small and shows a weak T dependence, $d\rho_{ab}/dT$ exhibits a rapid increase below $T \sim 10$ K close to the low temperature scale of Kondo lattice behavior, $T^* \sim 8$ K. This suggests that further coherence develops among f electrons due to the formation of heavy quasi particles below this temperature. The absence of similar increase in $d\rho_c/dT$ and large ρ_{ab}/ρ_c suggest that the associated heavy fermions are only mobile within the ab -plane, but not along the c -axis. This is consistent with the recent band calculation which found that the dispersion along the ab -plane is narrow due to the $4f$ electron contribution in comparison with the one along the c -axis for many of the bands mostly coming from conduction electrons²⁶. We find the anomalies in $d\rho/dT$ at 40-50 K around the same temperature scale as for the reflection points in χ (Fig. 1 (b)) where χ starts to show further increase on cooling. This temperature scale can be regarded as the onset temperature of the Kondo lattice behavior.

A possible explanation for the large anisotropy would be the anisotropic hybridization between the conduction and f electrons *i.e.* the smaller hybridization along the c -axis. In this case, while $T_0 \sim 200$ K has its origin in the in-plane hybridization, the hybridization scale along the c -axis should be smaller. This may also explain why the coherence peak is observed only in ρ_{ab} . Indeed, the recent band calculation suggests the smaller hybridization along the c -axis in β -YbAlB₄²⁶. Although the lower symmetry in α -YbAlB₄ makes its band structure more complex, the general features such as anisotropic hybridization are expected to be similar to each other.

In addition, according to a recent theory on the electronic structure, a hybridization node is expected along the c -axis in α - and β -YbAlB₄ based on the local Yb site symmetry if the crystal field ground doublet is made solely of $|J_z = \pm 5/2\rangle$ ^{19,31}. In this case, the c -axis transport should mostly come from the conduction electrons and thus should have much larger conductivity because of almost no scattering by f -electrons. The resultant anisotropy of the resistivity should be large when the ground $|J_z = \pm 5/2\rangle$ state is dominant at low temperatures. If f electrons start populating the excited CEF levels on heating, the ratio ρ_{ab}/ρ_c should decrease because the node is no longer well defined. Indeed, as shown in Fig. 4 (a), ρ_{ab}/ρ_c has a large value below ~ 10 K, and rapidly decreases with a characteristic temperature scale close to the CEF gap energy of ~ 80 K¹⁹.

The above two theoretical indications strongly support the existence of the anisotropic hybridization. It is not likely that the Kondo lattice scale $T^* \sim 8$ K comes from the smaller hybridization scale along the c -axis because no feature is observed at ~ 8 K in ρ_c . Instead, as it is already discussed, $T^* \sim 8$ K should arise from the in-plane correlation among f electrons. To confirm this, Yb-Yb intersite correlation effect should be clarified through, for

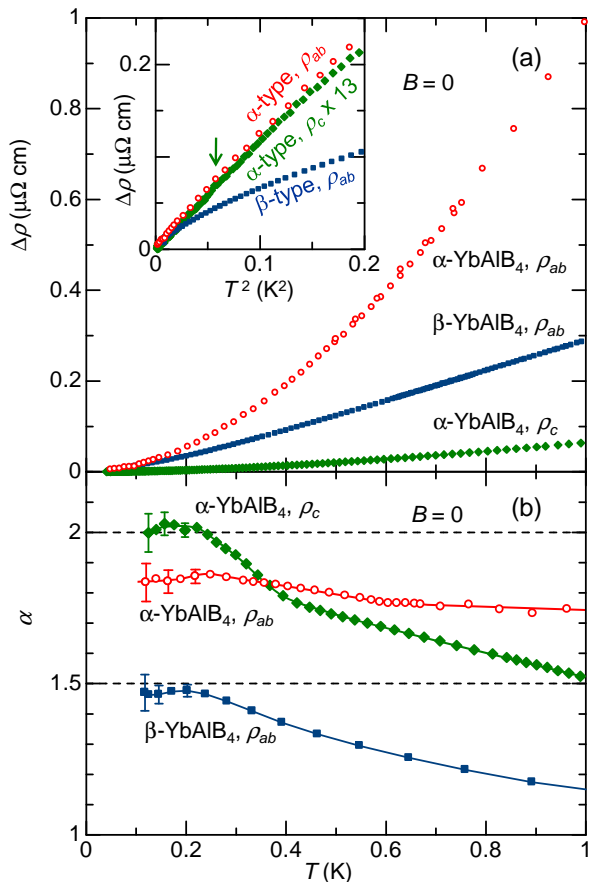


FIG. 5: (a) Temperature dependence of $\Delta\rho \equiv \rho - \rho_0$. Inset shows $\Delta\rho$ versus T^2 . Note that $\Delta\rho_c$ for α -YbAlB₄ is multiplied by a factor of 13 for clarity. The arrow indicate $T_F = 240$ mK estimated for ρ_c of α -YbAlB₄ by using the resistivity exponent α (see text). (b) The resistivity exponent α defined by $\Delta\rho = AT^\alpha$ (see text).

example, the Lu dilution study in Yb_{1-x}Lu_xAlB₄ systems.

The temperature dependent parts of the resistivity $\Delta\rho \equiv \rho - \rho_0$ at $T < 1$ K are shown in Fig. 5 (a). Here ρ_0 is the zero temperature limit of the resistivity, which was estimated by a power law fit of the low T data down to 35 mK (the detail is discussed later). ρ_0 are 9.4, 0.82 $\mu\Omega\text{cm}$ for ρ_{ab} , ρ_c of α -YbAlB₄, respectively (RRR ~ 20 and 70) and 0.49 $\mu\Omega\text{cm}$ for ρ_{ab} of β -YbAlB₄ (RRR ~ 250). The anisotropy in ρ_0 , which corresponds to $\rho_{ab}/\rho_c \sim 11$ in the lowest T , is almost the same as that of $\Delta\rho$ ($\Delta\rho_{ab}/\Delta\rho_c$) which is as large as 13 in the low T limit (Fig. 4 (a)). $\Delta\rho_{ab}$ of β -YbAlB₄ takes a value between $\Delta\rho_{ab}$ and $\Delta\rho_c$ of the α -phase. On the other hand, if we compare $\Delta\rho/\rho_0$, β -YbAlB₄ exhibits much larger value than those in α -YbAlB₄. For instance, $\Delta\rho_{ab}/\rho_0 = 0.85$ at $T = 1$ K in β -YbAlB₄ is ~ 10 times larger than the respective $\Delta\rho/\rho_0 = 0.11(\rho_{ab})$ and $0.08(\rho_c)$ for α -YbAlB₄. This cannot be explained only by the better sample quality in β -YbAlB₄, and thus the quantum criticality in β -YbAlB₄ should also

be responsible for the enhancement. Indeed, the application of the magnetic field, suppressing the criticality, decreases $\Delta\rho/\rho_0$ of β -YbAlB₄ to the same order as that in α -YbAlB₄. Note that even a α -YbAlB₄ sample with the highest RRR ~ 110 (estimated by ρ_c) does not exhibit superconductivity down to 35 mK (not shown).

To demonstrate the difference in the ground state of α - and β -YbAlB₄, we show the temperature dependence of the power law exponent α defined by $\Delta\rho = \rho_0 + A'T^\alpha$ (Fig. 5 (b)). α is obtained by using the equation $\alpha = d \log \Delta\rho / d \log T$. ρ_0 was determined using the best fitting result to the above equation that indicates the corresponding power law behavior in the widest temperature range from the lowest temperature. α is strongly dependent on ρ_0 , and its error due to 0.01% change in ρ_0 are shown in Fig. 5 (b). While the exponent α in β -YbAlB₄ is small $\lesssim 1.5$ at the low temperatures, those in α -YbAlB₄ are much larger and approaches the normal value of 2 expected for FL on cooling. This can be also confirmed in the plot against T^2 (inset of Fig. 5 (a)), where $\rho_c(T)$ of α -YbAlB₄ shows a linear dependence on T^2 below $T_{FL} \sim 240$ mK. The observation of $\alpha \sim 2$ in the lowest temperatures in addition to almost saturating χ and C_m/T below $T^* \sim 8$ K indicates that the ground state of α -YbAlB₄ is a Fermi liquid.

The T^2 -coefficient A defined by $\Delta\rho = \rho_0 + AT^2$ was estimated by the linear fit in the inset of Fig. 5 (a) below 240 mK. The obtained A values are 0.094 and 1.27 $\mu\Omega\text{cm} / \text{K}^2$ for ρ_c and ρ_{ab} , respectively. Kadowaki-Woods ratio A/γ^2 estimated by using these anisotropic A values are 5.8×10^{-6} and $7.8 \times 10^{-5} \mu\Omega\text{cm}(\text{K mol/mJ})^2$ for ρ_c and ρ_{ab} , respectively. Here γ is a low temperature limit of C/T , and in the present case, the value at 0.4 K (127 mJ/mol K²) was used. It is known that, the ratio A/γ^2 is close to $1.0 \times 10^{-5} \mu\Omega\text{cm}(\text{K mol/mJ})^2$ in many heavy fermion compounds of Kondo lattice systems³⁶. On the other hand, Tsujii *et al.* have suggested that the ratio is considerably smaller in intermediate valence systems, or equivalently, the systems with large orbital degeneracy N *i.e.* the system with a large hybridization scale T_0 compared to CEF splitting Δ ^{32,37}. In this case, the expected ratio is close to the typical value known for transition metals $A/\gamma^2 = 0.4 \times 10^{-6} \mu\Omega\text{cm}(\text{K mol/mJ})^2$, which is 25 times smaller than the above ratio for heavy fermions³⁵. To illustrate this, we show in Fig. 6, a full logarithmic plot of A versus γ (Kadowaki-Woods plot) for representative Ce and Yb based $4f$ electron systems³²⁻³⁴. A/γ^2 for most of the mixed valent materials or materials with large N (in Ce systems: $N = 6$ and in Yb systems: $N = 8$) is much smaller than the original Kadowaki-Woods ratio and has value of the order of $10^{-7} \mu\Omega\text{cm}(\text{K mol/mJ})^2$. Compared to these small values observed in mixed valence materials, the ratio obtained for ρ_c and ρ_{ab} of α -YbAlB₄ is much larger and close to the typical value for heavy fermions. In β -YbAlB₄, the ratio for ρ_{ab} also takes a similar value of $4.4 \times 10^{-5} \mu\Omega\text{cm}(\text{K mol/mJ})^2$ in magnetic field of 2 T along the c -axis^{7,9}. The large A/γ^2 in α -YbAlB₄ and β -YbAlB₄ ($B = 2$ T ||

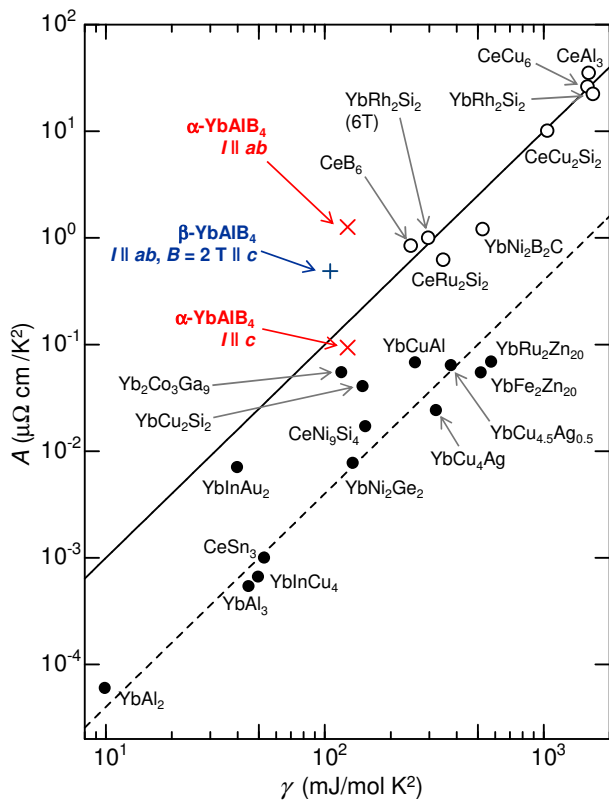


FIG. 6: T^2 -coefficient A of the resistivity versus the T -linear coefficient of the specific heat γ for both α - and β -YbAlB₄ as well as for other Ce and Yb based heavy fermions^{32–34}. The open circles denote Kondo lattice systems or the systems with crystal field ground state degeneracy $N = 2$. The closed circles denote mixed valent systems, Ce systems with $N = 6$ and Yb systems with $N = 8$. The solid line indicates the original Kadowaki-Woods ratio $A/\gamma^2 = 1.0 \times 10^{-5} \mu\Omega \text{ cm}(\text{K mol/mJ})^2$. The broken line corresponds to $A/\gamma^2 = 4.0 \times 10^{-7} \mu\Omega \text{ cm}(\text{K mol/mJ})^2$, which is the typical value in transition metals³⁵. The data of β -YbAlB₄ at $B = 2 \text{ T} \parallel c$ ^{7,9} is also shown.

c -axis) indicate that the system behaves like Kondo lattices at low temperatures rather than mixed valent materials. Interestingly, the ratio obtained for ρ_{ab} in both α - and β -YbAlB₄ is several times larger than the typical value for Kondo lattice systems. This deviation may come from material dependent properties such as dimen-

sionality and carrier concentration³⁸. Further analyses based on fermiology is required to clarify the origin of the enhancement in the Kadowaki-Woods ratio.

IV. CONCLUSION

Our detailed measurements have confirmed that both α -YbAlB₄ and β -YbAlB₄ exhibit Kondo lattice behavior with a small renormalized temperature scale of $T^* \sim 8 \text{ K}$ in addition to a large valence fluctuation scale of $\sim 200 \text{ K}$. Below $T^* \sim 8 \text{ K}$, α -YbAlB₄ forms a heavy Fermi liquid state with $\gamma \sim 130 \text{ mJ/mol K}^2$ in contrast to the unconventional quantum criticality observed in β -YbAlB₄. The Kadowaki-Woods ratio takes a typical value for Kondo lattice systems and considerably larger than those for mixed valent systems. This is consistent with the Kondo lattice behavior found in the temperature dependence of the susceptibility and specific heat. The large Wilson ratio more than 7 suggests that a ferromagnetic intersite coupling between Yb $4f$ -electrons and / or proximity to a valence quantum criticality, may be the origin of the Kondo lattice behavior. Furthermore, the large anisotropy observed in the resistivities suggests that hybridization between $4f$ and conduction electrons is much stronger within the ab -plane than along the c -axis. This strongly anisotropic hybridization and the large Wilson ratio are the keys to understand the unusual Kondo lattice behavior and heavy fermion formation in these mixed valence compounds. The future works including neutron scattering measurements and studies of Lu dilution effect in Yb_{1-x}Lu_xAlB₄ systems are necessary to clarify the origin of these unusual behaviors.

Acknowledgments

We thank N. Horie, E. C. T. O’Farrell, C. Petrovic, P. Coleman, A. H. Nevidomskyy, H. Harima, S. Watanabe, C. Broholm, K. Ueda and T. Sakakibara for supports and useful discussions. This work is partially supported by Grants-in-Aid (No. 21684019) from JSPS, by Grants-in-Aids for Scientific Research on Innovative Areas (No. 20102007, No. 21102507) from MEXT, Japan, by Global COE Program “the Physical Sciences Frontier”, MEXT, Japan, by Toray Science and Technology Grant.

* matsumoto@issp.u-toyko.ac.jp

† Present address: Department of Physics, College of Humanities and Sciences, Nihon University, Sakurajosui, Setagaya-ku, Tokyo 156-8550, Japan

‡ satoru@issp.u-tokyo.ac.jp

¹ N. D. Mathur, F. M. Grosche, S. R. Julian, I. R. Walker, D. M. Freye, R. K. W. Haselwimmer, and G. G. Lonzarich, Nature, **394**, 39 (1998).

² G. R. Stewart, Rev. Mod. Phys., **73**, 797 (2001).

³ H. Q. Yuan, F. M. Grosche, M. Deppe, C. Geibel, G. Sparn, and F. Steglich, Science, **302**, 2104 (2003).

⁴ H. v. Löhneysen, A. Rosch, M. Vojta, and P. Wölfle, Rev. Mod. Phys., **79**, 1015 (2007).

⁵ P. Monthoux, D. Pines, and G. G. Lonzarich, Nature, **450**, 1177 (2007).

⁶ P. Gegenwart, Q. Si, and F. Steglich, Nature Phys., **4**, 186 (2008).

⁷ S. Nakatsuji, K. Kuga, Y. Machida, T. Tayama, T. Sakak-

- ibara, Y. Karaki, H. Ishimoto, S. Yonezawa, Y. Maeno, E. Pearson, G. G. Lonzarich, L. Balicas, H. Lee, and Z. Fisk, *Nature Phys.*, **4**, 603 (2008).
- ⁸ K. Kuga, Y. Karaki, Y. Matsumoto, Y. Machida, and S. Nakatsuji, *Phys. Rev. Lett.*, **101**, 137004 (2008).
- ⁹ Y. Matsumoto, S. Nakatsuji, K. Kuga, Y. Karaki, N. Horie, Y. Shimura, T. Sakakibara, A. H. Nevidomskyy, and P. Coleman, *Science*, **331**, 316 (2011).
- ¹⁰ J. A. Hertz, *Phys. Rev. B*, **14**, 1165 (1976).
- ¹¹ T. Moriya, *Spin Fluctuations in Itinerant Electron Magnetism* (Springer, Berlin, 1985).
- ¹² A. J. Millis, *Phys. Rev. B*, **48**, 7183 (1993).
- ¹³ M. Okawa *et al.*, *Phys. Rev. Lett.*, **104**, 247201 (2010).
- ¹⁴ Z. Fisk, K. N. Yang, M. B. Maple, and H. R. Ott, *Valence Fluctuations in Solids* (North-Holland, New York, 1981) pp. 345–347.
- ¹⁵ R. T. Macaluso, S. Nakatsuji, K. Kuga, E. L. Thomas, Y. Machida, Y. Maeno, Z. Fisk, and J. Y. Chan, *Chem. Mater.*, **19**, 1918 (2007).
- ¹⁶ Y. Matsumoto, K. Kuga, N. Horie, and S. Nakatsuji, *J. Phys.: Conf. Ser.*, **273**, 012006 (2011).
- ¹⁷ S. H. Liu, C. Stassis, and J. K.A. Gschneidner, *Valence Fluctuation in Solids*, edited by L. M. Falicov, W. Hanke, and M. B. Maple (North-Holland, Amsterdam, 1981) p. 99.
- ¹⁸ A. L. Cornelius *et al.*, *Phys. Rev. Lett.*, **88**, 117201 (2002).
- ¹⁹ A. H. Nevidomskyy and P. Coleman, *Phys. Rev. Lett.*, **102**, 077202 (2009).
- ²⁰ E. C. T. O’Farrell, D. A. Tompsett, S. E. Sebastian, N. Harrison, C. Capan, L. Balicas, K. Kuga, A. Matsuo, K. Kindo, M. Tokunaga, S. Nakatsuji, G. Csányi, Z. Fisk, and M. L. Sutherland, *Phys. Rev. Lett.*, **102**, 216402 (2009).
- ²¹ H. v. Löhneysen, *J. Phys.: Condens. Matter*, **8**, 9689 (1996).
- ²² J. Custers *et al.*, *Nature*, **424**, 524 (2003).
- ²³ T. Tsuchida and W. E. Wallace, *J. Chem. Phys.*, **43**, 3811 (1965).
- ²⁴ A. H. Nevidomskyy and P. Coleman, *Phys. Rev. Lett.*, **103**, 147205 (2009).
- ²⁵ S. Watanabe and K. Miyake, *Phys. Rev. Lett.*, **105**, 186403 (2010).
- ²⁶ D. A. Tompsett, Z. P. Yin, G. G. Lonzarich, and W. E. Pickett, *Phys. Rev. B*, **82**, 235101 (2010).
- ²⁷ A. Malinowski, M. F. Hundley, C. Capan, F. Ronning, R. Movshovich, N. O. Moreno, J. L. Sarrao, and J. D. Thompson, *Phys. Rev. B*, **72**, 184506 (2005).
- ²⁸ Y. Ōnuki, Y. Furukawa, and T. Komatsubara, *J. Phys. Soc. Jpn.*, **53**, 2197 (1984).
- ²⁹ H. Fujii, T. Takabatake, and Y. Andoh, *J. Alloys Compd.*, **181**, 111 (1992).
- ³⁰ P. G. Niklowitz, G. Knebel, J. Flouquet, S. L. Bud’ko, and P. C. Canfield, *Phys. Rev. B*, **73**, 125101 (2006).
- ³¹ A. Ramires, P. Coleman, A. H. Nevidomskyy and A. M. Tsvelik, *private communication*.
- ³² N. Tsujii, H. Kontani, and K. Yoshimura, *Phys. Rev. Lett.*, **94**, 057201 (2005).
- ³³ M. S. Torikachvili, S. Jia, E. D. Mun, S. T. Hannahs, R. C. Black, W. K. Neils, D. Martien, S. L. Bud’ko, and P. C. Canfield, *Proc. Natl. Acad. Sci. U.S.A.*, **104**, 9960 (2007).
- ³⁴ T. D. Matsuda, N. D. Dung, Y. Haga, S. Ikeda, E. Yamamoto, T. Ishikura, T. Endo, T. T. R. Settai, and Y. Ōnuki, *Phys. Status Solidi B*, **247**, 757 (2010).
- ³⁵ M. J. Rice, *Phys. Rev. Lett.*, **20**, 1439 (1968).
- ³⁶ K. Kadowaki and S. B. Woods, *Solid State Commun.*, **58**, 507 (1986).
- ³⁷ N. Tsujii, K. Yoshimura, and K. Kosuge, *J. Phys. Condens. Matter*, **15**, 1993 (2003).
- ³⁸ A. C. Jacko, J. O. Fjærestad, and B. J. Powell, *Nature Phys.*, **5**, 422 (2009).